Separation Science and Technology
Publication details, including instructions for authors and subscription information:
http://www.informaworld.com/smpp/title~content=t713708471

Modeling Electroretention of Proteins during Electropolarization Chromatography

Amar B. Shah[a]; J. F. G. Reis[a]; E. N. Lightfoot[a]; R. E. Moore[b]
[a] DEPARTMENT OF CHEMICAL ENGINEERING, UNIVERSITY OF WISCONSIN, MADISON, WISCONSIN [b] DEPARTMENT OF COMPUTER SCIENCE, UNIVERSITY OF WISCONSIN, MADISON, WISCONSIN

To cite this Article Shah, Amar B. , Reis, J. F. G. , Lightfoot, E. N. and Moore, R. E.(1979) 'Modeling Electroretention of Proteins during Electropolarization Chromatography', Separation Science and Technology, 14: 6, 475 — 497
To link to this Article: DOI: 10.1080/01496397908068471
URL: http://dx.doi.org/10.1080/01496397908068471

SEPARATION SCIENCE AND TECHNOLOGY, 14(6), pp. 475–497, 1979

Modeling Electroretention of Proteins during Electropolarization Chromatography

AMAR B. SHAH, J. F. G. REIS, and E. N. LIGHTFOOT

DEPARTMENT OF CHEMICAL ENGINEERING

R. E. MOORE

DEPARTMENT OF COMPUTER SCIENCE
UNIVERSITY OF WISCONSIN
MADISON, WISCONSIN 53706

Abstract

An attempt is made to extend the understanding of electropolarization chromatography (EPC) by consideration of the nonlinear effects which dominate the system behavior for high polarizing fields. Of particular interest is the phenomenon of electroretention, a total immobilization of any protein above a finite, species-dependent, critical field strength. The modeling effort appears to have clarified the effects of high fields on many aspects of EPC, particularly the decrease in retardation with an increase in protein loading. It is unsuccessful in explaining electroretention because our model insufficiently predicts high degrees of concentration polarization. The basic reasons for this underestimation of polarization are not yet known, but they most probably reflect inadequate knowledge of transport and thermodynamic behavior of concentrated protein solutions. It is, however, also possible that the description of small-ion diffusion is oversimplified. Other effects like electroosmotic drying and a nonlinear electric field may also play a role in electroretention. It is recommended that further effort should be devoted primarily to the collection of transport and thermodynamic data of proteins at high concentrations, and systematic empirical investigation of this phenomenon.

INTRODUCTION

The main objective of this research is to increase the utility of electropolarization chromatography (EPC) or electrical field-flow fractionation, a relatively new separation process which appears attractive for fractionation of electrically charged polymers, at both the analytic and preparative levels. One of its potentially more attractive features is a very high selective solute retardation known as electroretention (ER) which is not yet understood. Since ER may be the key to successful large-scale application, it is important to understand this phenomenon better.

EPC, already described elsewhere (*1*), consists essentially of a channel of rectangular or circular cross-section bounded by semipermeable walls, bathed in a buffer solution, and subjected to a transverse electric field as described in Fig. 1. A carrier electrolyte flows continuously through

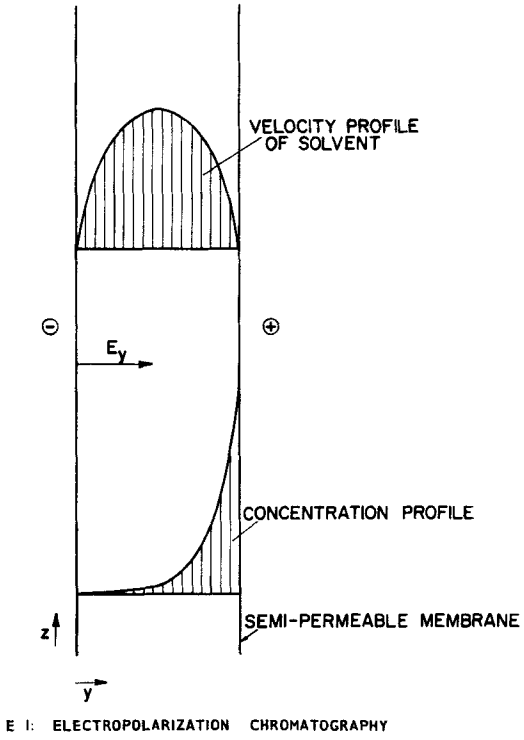

FIG. 1. Electropolarization chromatography.

the channel, and a pulse of a mixture of polyelectrolyte to be separated is introduced at the feed end ($z = 0$).

The electric field tends to concentrate the charged polymers, usually proteins, into the slow-moving fluid near a bounding surface and hence to increase their residence time. Reis (*2*) has developed a linear model which predicts that retardation should, for any geometry, depend only upon an electrical Péclet number

$$R_i = f(\varepsilon_i, \text{geometry}) \tag{1}$$

$$= \frac{\text{velocity of center of mass of species } i \text{ for zero field}}{\text{velocity of center of mass of species } i \text{ at finite field}}$$

where

$$\varepsilon_i = Rm_iE/D_{iw} \tag{2}$$

R = radius or half-thickness of channel (cm)

m_i = electrophoretic mobility of species i (cm^2/sec-V)

E = strength of polarizing field (V/cm)

D_{iw} = effective binary diffusivity of polarized solute (cm^2/sec)

For a rectangular channel

$$R_i = \varepsilon_i/3\left(\coth \varepsilon_i - \frac{1}{\varepsilon_i}\right) \tag{3}$$

while for channels of circular cross-section

$$R_i = \frac{\varepsilon_i I_1(\varepsilon_i)}{4I_2(\varepsilon_i)} \qquad \text{(where } I_1 \text{ and } I_2 \text{ are hyperbolic Bessel functions)} \tag{4}$$

according to this simplified theory.

Comparison of data (points and solid lines) with the predictions of Eq. (4) (dotted lines) for two proteins in Fig. 2 shows that the linear theory is adequate for sufficiently low voltages. However, for high fields, retardation increases much more rapidly than expected and, for the low protein loads represented here, retention is total above a critical field strength; no detectable protein leaves the column at supercritical fields even after many hours.

This total retention induced by the polarizing electrical field is called electroretention. As E_{critical} is species dependent, this appears to be a very attractive means of separation. The remainder of this paper is an attempt at a quantitative description of this electroretention phenomenon.

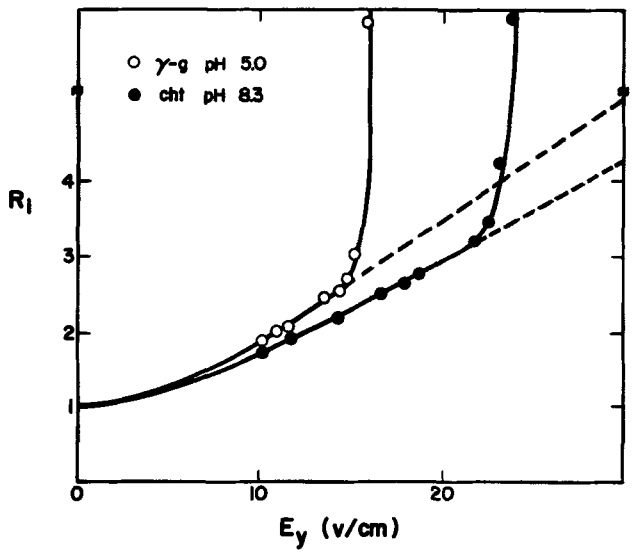

FIG. 2. Retardation and electroretention data for chymotrypsinogen A in Tris 0.001 *M* at pH 8.3. The electrical field was kept constant for 93 min after the injection and was then turned off. The flow rate was 12.5 μl/min.

DESCRIPTION OF ELECTRORETENTION

Electroretention has been observed for almost all the common globular proteins but, since we did not expect this phenomenon, it has yet to be systematically investigated. Available data are largely the result of chance. A typical case of ER is shown in Fig. 3, where at $E_y = 27$ V/cm the chymotrypsinogen is totally retained in the column and it leaves only when the electrical field is turned off. In some cases, as depicted in Table 1, hemoglobin is retained in the column for more than 10 hr. On turning the voltage to zero, the electroretained proteins quickly leave the column (the response time is typically half that of the average residence time). The type of observed ER peaks for different conditions of buffer solution, pH, voltage, carrier velocity, and the amount injected are summarized in Table 1. It is evident from this table that polyelectrolytes exhibit different behavior under the same pH, buffer solution, voltage, and carrier velocity. Although poorly understood, a few salient features of ER can be generalized:

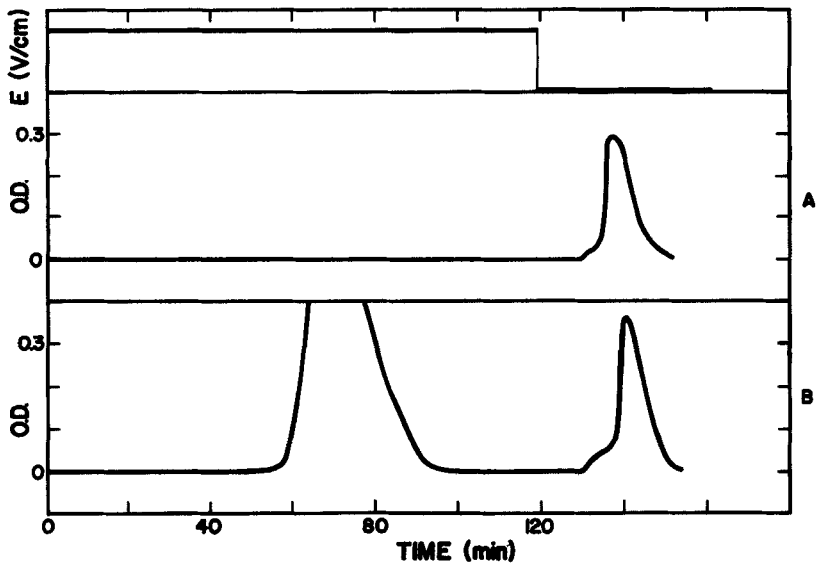

FIG. 3. Electroretention data on chymotrypsinogen A. The electrical field was 27 V/cm in both runs shown. In Run A, 50 μg of chymotrypsinogen A were injected; 250 μg were injected in Run B. This is a typical response to increases of loading.

(a) For all proteins examined (gamma-globulin, IgG, chymotrypsinogen, human serum albumin, hemoglobin, lactic acid dehydrogenase, cyanmet hemoglobin), ER takes place below 14.5 V/cm. [At high pH (8.3), however, we could not completely electroretain human serum albumin, even with 29 V/cm.] The interesting point is that the critical electrical field is species dependent. With the combination of EPC and ER carried out with a time programmed electric field, the separation of human IgG and IgM can be readily carried out (Fig. 4).

(b) The electroretained fraction can be totally recovered for some proteins and partially recovered for others.

(c) The ultrafiltration must be nearly zero, otherwise only partial or no ER is observed.

(d) As illustrated in Table 1, chymotrypsinogen is totally retained with 8.7 V/cm and only partial ER is observed with 29 V/cm for human serum albumin. However, for a mixture of these proteins, 5.8 V/cm will

TABLE 1

Electroretention of Proteins (membranes used: cellulose acetate and polysulfone)[a]

No.	Sample	Buffer	pH	Voltage (V)	Carrier velocity (μl/min)	Amount injected (μl)	Time elapsed before we put $V = 0$	Time for output after $V = 0$ (min)	Total or partial ER
1	CTG	Tris	8.3	20	12.3	10	60 min	8	Partial ER
	CTG	Tris	8.3	30	12.3	10	230	8	Total ER
	CTG	Tris	8.3	50	12.3	10	240 min	9	Total ER
	CTG	Tris	8.3	100	12.3	10	600 min	22	Total ER
2	G.G.	Tris	8.95	5	26	7	95 min	7.5	Partial ER
	G.G.	Tris	8.95	10	29	7	145 min	7	Partial ER
	G.G.	Tris	8.95	15	29	7	15 hr	7	Almost total ER
3	Hb	Tris	8.3	10	12.3	89 μg	270 min	5	Partial ER
	Hb	Tris	8.3	−20	12.3	10	10 hr	7	Almost total ER
	Hb	Tris	7.4	25	10 mg/m	10	10 hr	—	Total ER
4	HbCN	Phosphate	6.7	− 7	38	10	120 min	4	Partial ER
	HbCN	Phosphate	6.7	30	19	10	35 min	7	Total ER
5	HSA	Tris	8.3	100	12.3	10	80 min	10	Partial ER
6	IgG	Tris	8.95	25	13.3	7	60 min	5	Total ER
	IgG	Tris	8.3	30	12.3	10	115 min	6	Total ER
	IgG	Tris	8.3	50	12.3	20 μg	63 min	7	Total ER
7	L.D.H. mixture	Tris	8.35	50	12.3	5	33 min	11	Total ER
8	0.5 CTG + 0.5 HSA	Tris	8.3	20	12.3	10	130 min	—	Total ER

[a] CTG = chymotrypsinogen, G.G. = gamma globulin, Hb = hemoglobin, HbCN = cynamet-hemoglobin, HSA = human serum albumin, L.D.H. = lactic acid dehydrogenase.

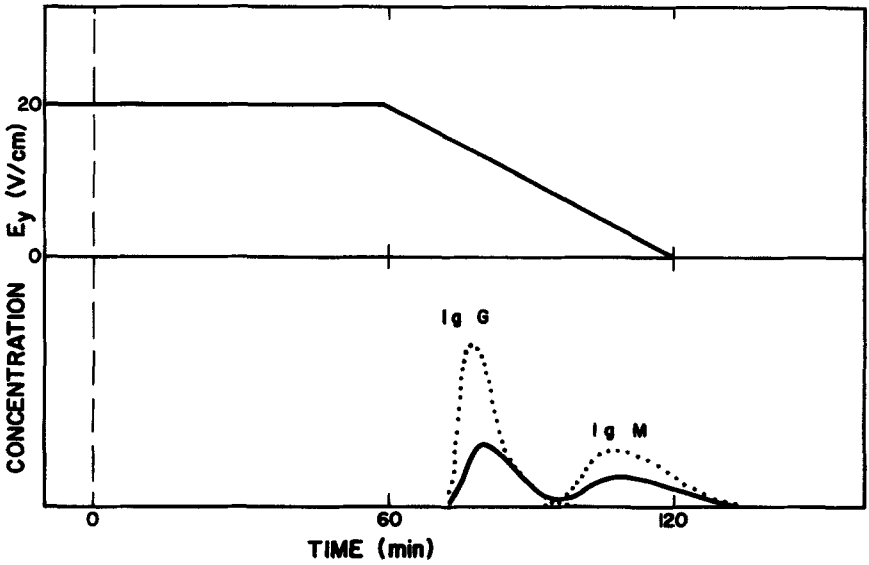

FIG. 4. Separation of IgM from IgG. The full line corresponds to the mixture and the dotted lines correspond to separate injections of the components of the mixture.

cause total ER. This indicates that some sort of interaction between the polyelectrolytes must be present.

(e) Generally, a loading effect is observed, i.e., above a certain mass of protein feed the electroretained fraction decreases. For example, if 50 μg of chymotrypsinogen A is injected into a 50-cm long, 0.4-mm diameter polysulfone hollow fiber at 27 V/cm, total ER is observed. However, for a 250-μg injection of chymotrypsinogen A is only partially retained at 27 V/cm (Figs. 3A and 3B).

(f) The necessary electrical field for electroretention is lowest when the protein is at its isoelectric point. For example, hemoglobin (isoelectric point = 6.7) can be totally retained in a phosphate buffer at pH = 6.4 with 10 V/cm, whereas in a Tris buffer at pH = 7.4, 20 V/cm is required.

All these empirical observations must be used in the search for possible mechanisms of ER. We will inquire in this paper if the concentration dependence of transport properties is enough to explain ER. In particular, the electromigration of polyelectrolytes toward the membrane gives rise

to a concentration gradient. The viscosity of macromolecules increases exponentially with concentration, whereas the diffusion coefficient decreases. Therefore, the spatial variation of viscosity and diffusion coefficient will contribute to a very strong polarization of the protein. The mathematical model developed below for varying transport properties will be used to determine if this strong polarization is able to justify ER.

MATHEMATICAL MODELS

Introduction

In this section we develop a model for ER. It must be recognized at the outset, however, that this process is quite complex, and that very few transport data exist for concentrated protein solutions. Hence a step-by-step approach is used, as outlined below.

Much of the complexity of the mathematical description of ER in hollow fibers results from the combination of the one-dimensional electrical field with the cylindrical fiber geometry and the axi-symmetric flow. It was shown by Reis et al. (*1*) that curvature effects are very small in the range of practical interest—polarization Péclet numbers (ε_i) over about 10. Moreover, Giddings (*3*) has observed ER in a planar geometry. On the basis of this observation it was decided to use a much simpler planar geometry in modeling ER.

The second major source of complexity is the nonlinearity of the generalized Stefan-Maxwell equations describing the combined effects of concentration diffusion and electromigration of protein and supporting electrolytes. The second step of our analysis was, therefore, to carry out a steady-state one-dimensional analysis of polarization in a model system consisting of one anionic protein species in a single salt. The results of this study are described in some detail in the section below. They may be summarized as indicating negligible polarization of the small electrolytes relative to that of the protein itself. Since polarization of small ions introduces considerable complexity into higher levels of modeling, it will be neglected.

In order to see whether the concentration dependence of the transport properties [viscosity (μ) and protein–water diffusion coefficient (D_{iw})] can explain ER, a steady-state one-dimensional model is first considered because it is mathematically more tractable than the real situation. The more realistic unsteady two-dimensional model for a pulse feed is then described.

Polarization of Low Molecular Weight Electrolytes

In the constant-property model of Reis (*1*, *2*) it was assumed that all low-molecular-weight solutes, including both buffer and supporting electrolyte, were maintained essentially at bulk concentration throughout the protein boundary layer. Since rather low electrolyte concentrations are used in EPC, it was thought necessary to test the validity of this assumption, and it was decided to do this using the simplified situation described in Fig. 5.

This model system consists of a simple protein anion ($P^{-\nu_P}$) in an elec-

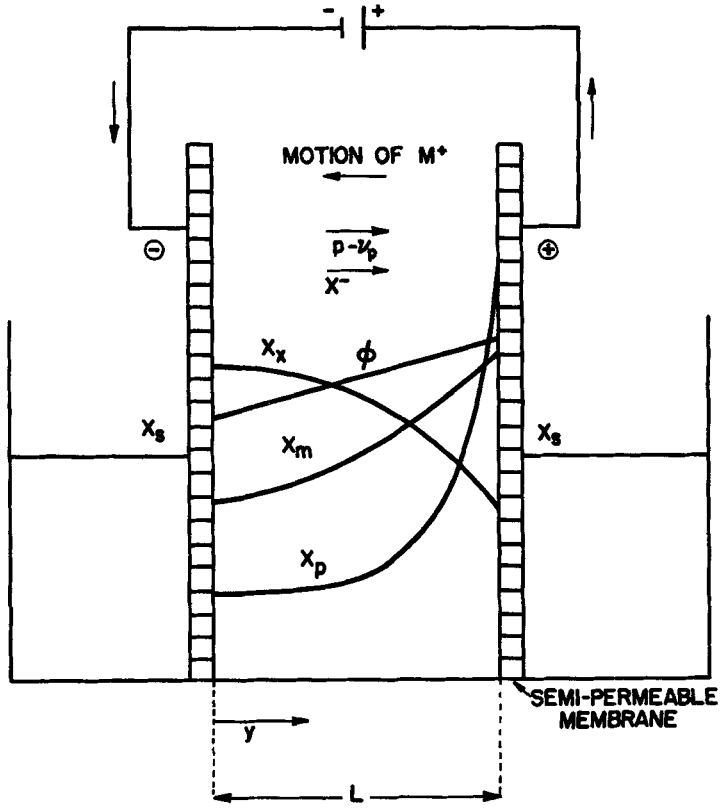

FIG. 5. Concentration polarization. The protein anion ($P^{-\nu_P}$) and the monovalent anion (X^-) migrate toward the anode whereas the monovalent cation (M^+) migrates toward the cathode.

trolyte containing only a monovalent anion (X^-) and a monovalent cation (M^+) in water (W). The three species are confined between two large parallel membranes freely permeable to M^+ and X^- but totally impermeable to the protein. Outside each of the bounding membranes is a solution of MX at uniform concentration X_s.

For convenience, X_M is set equal to a fixed value X_{M0} and the electric potential to ϕ_0 at $y = 0$, one bounding surface. In addition, all activity coefficients are set equal to unity and convective transport is neglected.

The description of this system is given by:

(a) A continuity equation for each ion.
(b) A diffusion equation for each ion.
(c) Boundary conditions.

The assumptions made in this analysis are:

(a) Electroneutrality is preserved.
(b) Transport properties are constant.
(c) Here, the pressure gradients are negligible.
(d) The operation is at steady state.
(e) Each ion is diffusing in a binary system with water as the second component.

For the very dilute solutions of interest here, the pseudobinary Nernst-Planck formulations (*4*) suffice. These equations follow.

Continuity Equations

At steady state, the molar fluxes of M and X are constant, whereas that of the protein is zero because the membrane is totally impermeable to the protein:

$$N_M = \text{constant} \tag{5}$$

$$N_X = \text{constant} \tag{6}$$

$$N_P = 0 \tag{7}$$

$$N_M - N_X = I \tag{8}$$

Diffusion Equations

The Stefan-Maxwell equations reduce to

$$0 = \frac{dX_P}{dh} - X_P \nu_P \frac{d\phi}{dh} \tag{9}$$

$$-1 = \frac{dX_X}{dh} - X_X\frac{d\phi}{dh} \tag{10}$$

$$-R = \frac{dX_M}{dh} + X_M\frac{d\phi}{dh} \tag{11}$$

$$\sum X_i = 1 \tag{12}$$

Electroneutrality

Electroneutrality requires that

$$X_M = X_X + \nu_P X_P \tag{13}$$

Boundary Conditions

(a) At $h = 0$,

$$X_M = X_{M0};\ X_P = X_{P0};\ X_{X0} = X_{M0} - \nu_P X_{P0}$$
$$\phi = \phi_0 = 0;\ X_M X_X = X_s^2 \tag{14}$$

(b) At $h^* = LN_X/cD_{X,W}$

$$X_M X_X = X_s^2 \tag{15}$$

Integrating Eqs. (9) to (11) and using (13) gives

$$X_P = X_{P0}\exp(\nu_P\phi) \tag{16}$$

$$X_M - X_{M0} = -\left[\frac{1+R}{2}\right]h + \left[\frac{\nu_P - 1}{2}\right](X_P - X_{P0}) \tag{17}$$

$$X_X - X_{X0} = -\left[\frac{\nu_P + 1}{2}\right](X_P - X_{P0}) - \left[\frac{1+R}{2}\right]h \tag{18}$$

$$h = A(X_P)^B + \frac{(\nu_P^2 - 1)X_P}{\nu_P(1-R) - (1+R)} - \frac{(X_{P0} + X_{M0} + X_{X0})}{(1+R)} \tag{19}$$

where

$$A = \left[\frac{(X_{P0} + X_{M0} + X_{X0})}{(1+R)} - \frac{(\nu_P^2 - 1)X_{P0}}{\nu_P(1-R) - (1+R)}\right]\frac{1}{(X_{P0})^B} \tag{20}$$

$$B = \frac{(1+R)}{(1-R)}\frac{1}{\nu_P} \tag{21}$$

The above equation is implicit in the concentration of protein, and therefore the desired concentration profiles must be determined numeri-

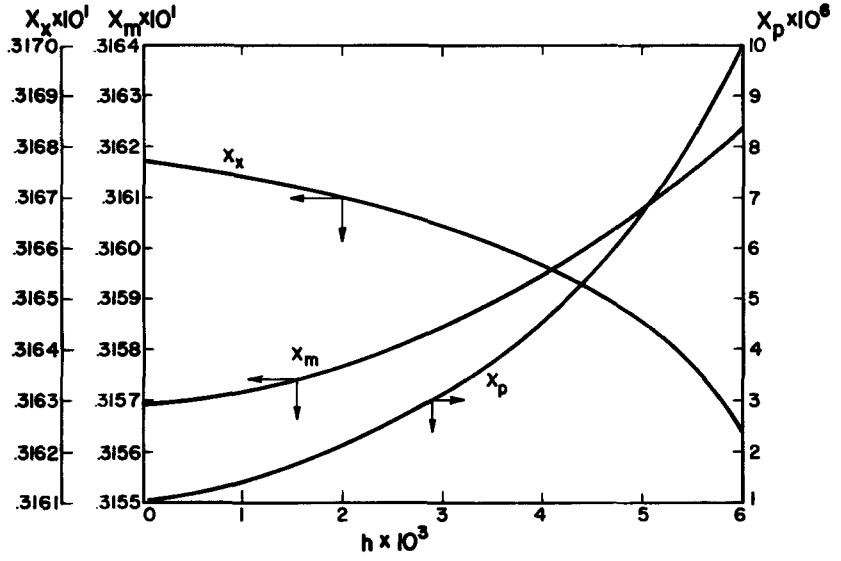

FIG. 6. Concentration profiles for a polarized cell.

cally. Typical values of L, X_s, I, etc. of practical interest to EPC are

$$X_s = 3.162 \times 10^{-2}$$
$$L = 0.05 \text{ cm}$$
$$c = 5.55 \times 10^{-2} \text{ gmoles/cm}^3$$
$$I = 10^{-5} \text{ A/cm}^2$$
$$D_{X,W} = 10^{-8} \text{ cm}^2/\text{sec}$$
$$N_X = I/2 = 5.2 \times 10^{-11} \text{ g-equiv/cm}^2\text{-sec}$$
$$h = 4.7 \times 10^{-3}$$

A typical concentration profile for these conditions is shown in Fig. 6. Here the protein mole fraction at the anodic boundary layer is 10^{-5} and the external salt mole fraction is 3.162×10^{-2}. As illustrated in Fig. 6, the change in the concentration of M is 0.18%, of X is 0.17%, whereas that of P is 900%. If our assumptions of electroneutrality etc. are valid, this implies that the polarization of the salt can be neglected in our subsequent analyses.

One-Dimensional Variable Transport-Property Model

Here we begin investigating the effects of finite concentration on EPC. To do this, we consider continuous feed of a protein solution to the planar

system of Fig. 1. A protein boundary layer (B.L.) builds up on the anodic boundary of the system as shown, and once steady state has been established, this B.L. becomes one-dimensional. It is our purpose to determine the retardation coefficient of the protein as defined by Eq. (1).

In this preliminary investigation only concentration dependence of viscosity (μ) and the protein–water mutual diffusion coefficient (D_{iw}) are taken into account. Furthermore, we approximate the concentration dependence of these quantities by

$$\frac{1}{\mu} = \begin{cases} 100[1.11 - (0.054)H + (6.7 \times 10^{-4})H^2], & \text{if } H < 41 \\ \dfrac{100}{\exp[0.00244H^2]}(1/\text{poise}), & \text{if } H \geq 41 \end{cases} \tag{22}$$

$$\frac{D_{PW}}{D_0} = \frac{\tanh(21.3\phi_P)}{(21.3)\phi_P} \tag{23}$$

where

$$H = [3.888 \times 10^5]X_P$$

$$D_0 = 6.8 \times 10^{-7}\ \text{cm}^2/\text{sec}$$

$$\phi_P = \frac{(93{,}333.33)X_P}{(70{,}000)X_P + 18[0.94 - X_P] + 1.85}$$

The data for viscosity (Eq. 22) were generated by Kozinski (*5*) for his B.L. analysis of bovine serum albumin, and they seem to be representative of what we might expect for globular proteins. The diffusion data were (Eq. 23) obtained by Keller et al. (*6*) for both bovine serum albumin and hemoglobin. Our calculations may therefore be considered as modeling bovine serum albumin.

As mentioned before, viscosity and diffusion variations are analyzed because of their obvious bearing on system behavior. Before going into the detailed mathematical analysis of the effect of variable viscosity and diffusivity, it is important to note that other transport and thermodynamic effects could have been considered:

(a) *Protein mobility*: There are little data on the concentration dependence of protein mobility in our concentration range. However, it is shown by Möller et al. (*7*) that above a certain concentration the electric mobility approaches an asymptotic value.

(b) *Small-ion transport*: Based on the results of the previous section, the polarization of small ions is neglected. Since the small ions carry the bulk of the current, this is equivalent to assuming that the electric field

is constant. We do not have any data to judge the validity of this assumption.

(c) *Solution density*: Kozinski (*5*) has shown that variations in solution density are a second-order effect, and therefore they are assumed to be a constant.

(d) *Phase transitions*: Here we have implicitly assumed that the protein remains in solution. There may be a phase transition (protein in solution→ protein gel) which we did not take into account.

When all these assumptions have been made, the system description for the steady-state one-dimensional model reduces to:

(a) *One Continuity Equation*:

$$N_{PY} = \text{constant} = 0 \text{ (impermeable membrane)} \tag{24}$$

where N_{PY} is the molar flux of protein in the y-direction.

(b) *One Diffusion Equation*:

$$N_{PY} = -c\left[D_{P,W}\frac{dX_P}{dy} - m_P X_P \frac{d\phi}{dy}\right] \tag{25}$$

(c) *Equation of Motion*:

The equation of motion for forced convection along the z-direction becomes

$$0 = -\frac{\partial P}{\partial z} - \frac{\partial \tau_{yz}}{\partial y} \tag{26}$$

with the boundary condition that

$$V_z = 0 \quad \text{at} \quad y = 0, L \tag{27}$$

(d) *Material Balance*:

On integrating Eq. (25) we obtain

$$X_P - X_{P,L} = \int_{y=L}^{y} \frac{m_P X_P E_y}{D_{P,W}}\, dy \tag{28}$$

The convective velocity profile can be obtained by solving Eq. (26).

$$V_z = \frac{(P_0 - P_Z)}{Z}\left[\left[\frac{\int_0^L (y/\mu)\, dy}{\int_0^L (1/\mu)\, dy}\right]\int_L^y \frac{dy}{\mu} - \int_L^y \frac{y\, dy}{\mu}\right] \tag{29}$$

The dimensionless velocity of the center of mass and the retardation coefficients are described earlier as

$$R_P = \frac{2}{3} V_0 \frac{\int_0^L X_P \, dy}{\int_0^L X_P v_z \, dy} \tag{1}$$

The above equations must be solved numerically, and this must be done for situations of practical interest. These were chosen as

$$E = 0 \text{ to } 30 \text{ V/cm}$$
$$M = 5.6 \times 10^{-9} \text{ to } 5.6 \times 10^{-11} \text{ gmole}$$
$$L = 0.05 \text{ cm}$$
$$m_P = 6 \times 10^{-5} \text{ cm}^2/\text{V-sec}$$
$$V_0 = 0.1 \text{ cm/sec}$$

These are the ranges of E and L when ER is observed.

The retardation coefficient for different amounts of protein as a function of electric field (E_y) are tabulated in Table 2 and illustrated in Fig. 7. The retardation coefficient increases exponentially when $M = 5.6 \times 10^{-11}$ gmole, but the retardation coefficient is nearly equal to Reis' (*2*) model (i.e., for constant μ and D_{iw}) when $M = 5.6 \times 10^{-9}$ gmole. This explains one aspect of loading which is explained in Fig. 7. Retardation Curves A, B and C in Fig. 7 are for feed loads of 5.6×10^{-11}, 5.6×10^{-10},

TABLE 2
Retardation Coefficients for One-Dimensional Case[a]

E_y (V/cm)	R (μ and D constant), Reis model	R		
		$M = 5.6 \times 10^{-9}$	$M = 5.6 \times 10^{-10}$	$M = 5.6 \times 10^{-4}$
1	1.287	1.29	1.31	3.46
2	1.902		2.07	
3	2.599		3.14	
4	3.317		4.56	
5	4.043	4.07	6.51	60.10
10	7.702	8.06	22.87	230.94
15	11.37		54.69	
20	15.04	17.02	95.93	
25	18.72		151.2	
30	22.39	28.2	213.4	

[a] R_p = retardation coefficients, M = amount injected (gmoles), E_y = electric field in y-direction (V/cm).

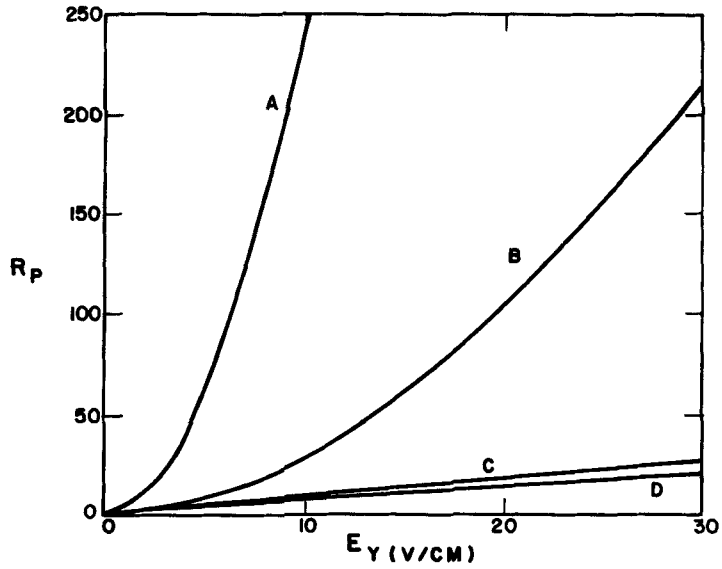

FIG. 7. Retardation coefficients of bovine serum albumin for the steady-state, one-dimensional model (Curve A, mass = 5.6×10^{-11} gmole; Curve B, mass = 4.6×10^{-10} gmole; Curve C, mass = 5.6×10^{-9} gmole). Curve D is the prediction of the linear model for constant transport properties.

and 5.6×10^{-9} gmole, respectively. Curve D corresponds to the R_P vs E_y for the linear model [i.e., μ and $D_{P,W}$ are constant: Reis (*2*) model]. In the case of Curves A and B, R_P increases very rapidly. Moreover, Curves A, B, and C explain the fact (discussed in the section entitled "Description of Electroretention") that for a particular value of E_y, R_P decreases with an increase in the amount injected.

These results are promising because they illustrate some key features of EPC. However, these results are valid only for a one-dimensional steady-state condition corresponding to continuous feed. To show that the spatial variations μ and D_{iw} are responsible for ER, a detailed unsteady-state two-dimensional model is in order. Although mathematically much more complex, it is necessary to delve into the intricacies of the mechanism because they might have surprises for us.

Two-Dimensional Unsteady-State Variable Property Model

The relatively simple variable-property model of the last section appears to exhibit the known features of ER reasonably well, but this description

cannot be considered definitive because it is not affected by the axial dispersion experienced by differential feed pulses. Accordingly, in this section the variable property model is extended to this more realistic situation.

The system analyzed differs only in the replacement of continuous feed by a square pulse input of protein. An electrically conducting solution flows along the z-direction with an electric field in the y-direction and square pulse of protein is fed at $z = 0$.

The equations governing the system are (a) equation of diffusion for protein and (b) equation of motion. The equations describing the system follow.

Diffusion Equation

$$\frac{\partial C_P}{\partial t} + \mathbf{V}\cdot\nabla C_P = \nabla\cdot D_{P,W}\nabla C_P \tag{30}$$

$$\frac{\partial C_P}{\partial t} + \left[V_z - \frac{\partial D_{P,W}}{\partial z}\right]\frac{\partial C_P}{\partial z} + \left[V_y - \frac{\partial D_{P,W}}{\partial y}\right]\frac{\partial C_P}{\partial y} = D_{P,W}\left[\frac{\partial^2 C_P}{\partial y^2} + \frac{\partial^2 C_P}{\partial z^2}\right] \tag{31}$$

Equation of Motion

$$0 = -\frac{\partial P}{\partial z} - \frac{\partial \tau_{yz}}{\partial y} \tag{32}$$

Boundary Conditions

$$V_z = 0 \quad \text{at} \quad y = 0, L \text{ (no slip condition)} \tag{33}$$

$$V_y C_P = D_{P,W}\frac{\partial C_P}{\partial y} \quad \text{at} \quad y = 0, L \text{ (impermeable membrane)} \tag{34}$$

Initial Condition at $t = 0$, $C = C_{input}$ for all y and from $z = 0$ to $z = z^*$. (The initial condition corresponds to uniform distribution of the protein solution from $z = 0$ to $z = z^*$.)

Clearly the integration of these equations is a nontrivial problem. The diffusion equation is a nonlinear parabolic partial differential equation and can be solved by finite difference techniques (i.e., discretizing the y, z, and t coordinates). The stability of this method (*8*, *9*) is improved by the proper choice of mesh sizes along the y, z, and t axes.

The above equations have been solved for conditions of practical interest. These are:

$E_y = 20, 30$ V/cm
$M = 7.1 \times 10^{-10}, 14.2 \times 10^{-10}$ gmole
$L = 0.05$ cm
$m_P = 6 \times 10^{-5}$ cm^2/V-sec
$V_0 = 0.1$ cm/sec

The dimensionless velocity of the center of mass and the retardation coefficient as a function of time are tabulated in Table 3. The values of R_P are illustrated in Fig. 8. The values of R_P are smaller than those observed experimentally (Fig. 2). The model does not predict the immobilization of albumin.

However, we do not experimentally observe ER of albumin at high pH. Therefore the fact that the model fails to predict immobilization is not surprising. The viscosity data for albumin predicts protein gelation at 42 g/100 cc. If this is decreased to 36 g/100 cc, we can predict ER. We used the data for albumin because we felt that they are representative of globular proteins and it is one of the few proteins for which reliable data are available.

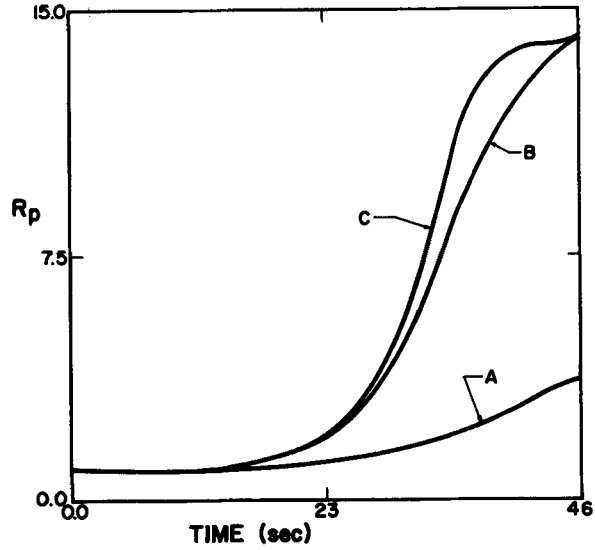

FIG. 8. Retardation coefficients of bovine serum albumin for the two-dimensional, unsteady-state model (Curve A, $E = 20$ V/cm, mass $= 7.1 \times 10^{-10}$ gmole; Curve B, $E = 30$ V/cm, mass $= 7.1 \times 10^{-10}$ gmole; Curve C, $E_y = 30$ V/cm, mass $= 14.2 \times 10^{-10}$ gmole).

TABLE 3
Retardation Coefficients

t (sec)	R_P at $E_y = 20$ V/cm and $M = 7.1 \times 10^{-10}$	R_P at $E_y = 30$ V/cm and $M = 7.1 \times 10^{-10}$	R_P at $E_y = 30$ V/cm and $M = 14.1 \times 10^{-10}$
0.0	1.0	1.0	1.0
0.5	1.052	.990	.986
1.0	1.028	.974	.968
1.5	1.013	.964	.957
2.0	1.004	.955	.947
2.5	.996	.947	.938
3.0	.990	.939	.930
3.5	.983	.932	.922
4.0	.977	.925	.915
5.0	.965	.915	.905
6.0	.955	.911	.900
7.0	.950	.912	.901
8.0	.948	.919	.909
9.0	.950	.931	.921
10.0	.953	.947	.938
11.0	.958	.968	.960
12.0	.966	.995	.989
13.0	.975	1.029	1.025
14.0	.987	1.069	1.069
15.0	1.002	1.119	1.123
16.0	1.018	1.178	1.187
17.0	1.038	1.250	1.265
18.0	1.061	1.336	1.359
19.0	1.088	1.438	1.472
20.0	1.117	1.561	1.608
22.0	1.189	1.881	1.964
24.0	1.278	2.318	2.471
26.0	1.387	2.926	3.183
28.0	1.520	3.727	4.181
30.0	1.680	4.791	5.592
32.0	1.870	6.212	7.566
34.0	2.093	8.006	10.038
36.0	2.348	9.733	12.029
38.0	2.634	10.894	13.232
40.0	2.949	11.983	13.748
42.0	3.293	13.073	13.905
44.0	3.658	13.635	13.942
46.0	3.838	14.145	14.012

It will be very useful to see whether this model predicts ER for proteins like IgG and Hb. Unfortunately, extensive transport data at high concentration for other proteins are not available.

This model does predict that it is difficult to electroretain albumin at the conditions where the data apply, and it gives us some clues to the mechanism of ER.

It is apparent that neither the one- nor two-dimensional models predicts ER, and it is probable that this failure results from the inability of either model to predict precipitation.

FURTHER DISCUSSION OF ELECTRORETENTION

The numerical modeling effort of the last two sections appears to describe the effects of viscosity and diffusivity variations, at least qualitatively.

The predicted decrease of R_P with an increase in protein loading has been found experimentally by Chiang et al. (*10*), and it would be useful to compare theory and experiment quantitatively. This will require a characterization of fiber electrical properties.

Not even the two-dimensional model predicts protein saturation near the wall, but experimental observations, on the other hand, show strong evidence of saturation as a characteristic feature of the ER process. Reasons for this underestimation are not known, but they probably reflect inadequate knowledge of the transport behavior of concentrated proteins.

The discrepancy between theory and experiment can also be attributed to the assumptions made in this analysis. These assumptions and other factors which might be responsible for ER are discussed below:

(a) In our model studies, electrophoretic mobility is assumed to be a constant. However, it is very sensitive to pH and is roughly proportional to the inverse of the square root of ionic strength. The functional dependence of mobility on pH, ionic strength, and concentration are important points neglected in our analysis.

(b) The solubility estimates of the protein are based on the viscosity data at normal ionic strength. They might be in error, and more reliable solubility data are desired.

(c) The precipitated protein may behave like a secondary membrane, and under an applied voltage this could give rise to electroosmotic drying.

(d) The assumption of constant electric field may not be valid near

the membrane, and this nonuniformity in electric field may increase the degree of polarization.

(e) It is possible that the pseudobinary diffusion assumption neglected important aspects of small-ion transport in this complex system. In particular, polarization of the buffer might be important.

(f) The large protein-to-salt ratio might increase the electrophoretic mobility and decrease the diffusion coefficient. At this high concentration there is also a possibility of protein-protein association. As there are no data to support this hypothesis, it requires careful experimental investigation.

CONCLUSIONS AND RECOMMENDATIONS

Various mathematical models are developed to explain the mechanism of ER. The one-dimensional steady-state model with varying transport properties predicts high retardation coefficients and explains one aspect of the loading effect. For final confirmation, an unsteady-state two-dimensional model for a pulse feed is developed. This model does not predict ER of albumin, and this agrees with experimental observation. This model cannot be tested for other proteins because extensive transport data for other proteins are not available. However, these models give us an insight to the possible mechanism of ER.

This study indicates that further work in this area should be directed toward the collection of extensive transport and thermodynamic properties of proteins at high concentration. With these properties a general model, including other effects like electroosmosis, nonuniform electric conductivity, and polarization of buffer, can be developed.

As ER offers a unique method for separating polyelectrolytes, it should be thoroughly understood if the practical potential of EPC is to be realized.

Acknowledgments

The authors are indebted to the National Science Foundation for financial support. The comments from Dr. W. E. Stewart, Dr. Randy Seright, and Dr. Simon Hobbs are deeply appreciated.

SYMBOLS

c total concentration (gmoles/cm^3)
$m_i E_y L/2D_{im}$

C_i concentration of species i (gmoles/cm^3)
D_{iw} mutual i–water diffusion coefficient (cm^2/sec)
E_y electric field in the y-direction [V/cm]
F Faraday's constant
h $yN_x/cD_{x,w}$
I current density (A/cm^2)
L distance between the parallel membranes (cm)
m_i electric mobility of species i (cm^2/V-sec)
M monovalent cation
M total amount of protein injected at $t = 0$ (gmoles)
N_i molar flux of species i (gmoles/cm^2-sec)
P_0 and P_z pressures at $z = 0$ and $z = L$, respectively
R $(N_m/N_x)/(D_{x,w}/D_{m,w})$
R_g gas constant
R_i retardation coefficient of species i
t time (sec)
T temperature
V_y, V_z velocity in the y and z direction (cm/sec)
V_0 maximum velocity at a particular z in the z direction (cm/sec)
X monovalent anion
X_i mole fraction of species i
y distance along y-direction (cm)
z distance along z-direction (cm)
α_i dimensionless velocity of the center of mass
ν_P charge on the protein molecule
Φ electric potential (V)
ϕ_i volume fraction of species i
ϕ Φ/R_gT
μ viscosity (g/cm-sec)
τ_{yz} yz component of shear stress

Subscripts

i M = cation
X = anion
P = protein
W = water
S = for anion or cation in the external solution
0 value at $y = 0$

REFERENCES

1. J. F. G. Reis, D. Ramkrishna, and E. N. Lightfoot, "Convective Mass Transfer in Presence of Polarizing Fields: Dispersion in Hollow-Fiber Electropolarization Chromatography," *AIChE J.*, In Press.
2. J. F. G. Reis, Ph.D. Thesis, University of Wisconsin, Madison, Wisconsin, 1976.
3. J. C. Giddings, Private Communication.
4. E. N. Lightfoot, *Transport Phenomena and Living Systems*, Wiley-Interscience, New York, 1974.
5. A. A. Kozinski, Ph.D. Thesis, University of Wisconsin, Madison, Wisconsin, 1971.
6. H. K. Keller, E. R. Canales, and S. I. Yum, "Traces and Mutual Diffusion Coefficients of Proteins," *J. Phy. Chem.*, *75*(3), 379–387 (1971).
7. W. J. H. M. Möller, G. A. J. Van Oss, and J. T. G. Overbeek, "Electrical Conductivity and Transference of Alkali Albuminates," *Trans. Faraday Soc.*, *57*, 312–337 (1961).
8. R. E. Moore, *Mathematical Elements of Scientific Computing*, Holt, Rinehart and Winston, New York, 1975.
9. D. Greenspan, *Discrete Numerical Methods in Physics and Engineering*, Academic, New York, 1974.
10. A. S. Chiang, E. H. Kimiotek, S. M. Langan, P. T. Noble, J. F. G. Reis, and E. N. Lightfoot, "Preliminary Experimental Survey of Hollow-fiber Electropolarization Chromatography," To Be Published.

Received by editor October 16, 1978